Diacetylenic Lipid Microstructures: Structural Characterization by X-ray Diffraction and Comparison with the Saturated Phosphatidylcholine Analogue†

Martin Caffrey,*,‡ Jacqueline Hogan,‡ and Alan S. Rudolph§

Department of Chemistry, The Ohio State University, 120 West 18th Avenue, Columbus, Ohio 43210, and Center for Biomolecular Engineering, Naval Research Laboratory, Washington, D.C. 20375-5000

Received August 7, 1990; Revised Manuscript Received October 25, 1990

ABSTRACT: Thermotropic and lyotropic mesomorphism in the polymerizable lecithin 1,2-ditricosa-10,12-diynoyl-*sn*-glycero-3-phosphocholine and its saturated analogue, 1,2-ditricosanoyl-*sn*-glycero-3-phosphocholine, has been investigated by wide- and low-angle X-ray diffraction of both powder and oriented samples and by differential scanning calorimetry. Previous studies have shown that the hydrated diacetylenic lipid forms novel microstructures (tubules and stacked bilayer sheets) in its low-temperature phase. The diffraction results indicate that at low temperatures fully hydrated tubules and sheets have an identical lamellar repeat size (d_{00l} = 66.4 Å) and crystalline-like packing of the acyl chains. Chain packing in the lamellar crystalline phase is hydration independent. A model for the polymerizable lecithin with (1) fully extended all-trans methylene segments, (2) a long-axis tilt of 32°, and (3) minimal chain interdigitation seems most reasonable on energetic grounds, is consistent with the diffraction data (to 3.93-Å resolution), and is likely to support facile polymerization. Above the chain "melting" transition the lamellar repeat of the polymerizable lipid increases to 74 Å. The conformational similarity between tubules, sheets, and the dry powder is corroborated by calorimetry, which reveals a cooling exotherm at the same temperature where tubules form upon cooling hydrated sheets. The data suggest that although a high degree of conformational order is a pertinent feature of tubules, this character alone is not sufficient to account for tubule formation. The conformation of the corresponding saturated phosphatidylcholine appears to be similar to that of other saturated phosphatidylcholines in the lamellar gel phase. Furthermore, above the main transition temperature, the dry, saturated lipid shows evidence of a P_δ phase (112 °C), whereas the diacetylenic lipid appears to exhibit a centered rectangular phase, R_α (55 °C).

The diacetylenic lipids, the lecithins in particular, have received increasing attention of late. From a purely physicochemical perspective, the structural consequences of introducing multiple C–C triple bonds in an otherwise fully saturated long-chain hydrocarbon has yet to be established. The diacetylenic lipids are polymerizable, which is interesting in its own right but additionally confers potential industrial and biotechnological utility to these materials (Regen et al., 1982; Hupfer et al., 1983; Johnston & Chapman, 1985; Johnston et al., 1983). A number of the diacetylenic lipids form unique morphologies such as cylinders, helices, and large domains of nonvesicular flat bilayers (Yager & Schoen, 1984; Schnur et al., 1987; Yager et al., 1985; Georger et al., 1987; Rudolph & Burke, 1987). The self-assembly of diacetylenic lipids into morphologies other than liposomes presents an opportunity to query the physical–chemical driving forces necessary for the self-assembly of a particular microstructure morphology.

In this study we examine the thermal and structural properties of the diacetylenic lipid, 1,2-ditricosa-10,12-diynoyl-*sn*-glycero-3-phosphocholine ($DC_{8,9}PC$)[1] and its saturated analogue, 1,2-ditricosanoyl-*sn*-glycero-3-phosphocholine (DTPC). The initial studies of the polymorphic phase behavior of the diacetylenic lipid revealed the formation of hollow, cylindrical microstructures called tubules (Yager & Schoen, 1984). The high aspect ratio of these structures, the potential for decoration with fluorophores, metals, polymers, etc., the ability to orient in high magnetic fields, and the utilization of the aqueous interior for encapsulation make tubules attractive candidates for technological applications (Schnur et

† This work was supported by a grant from the National Institutes of Health (DK36849), a University Exploratory Research Program Award (The Procter and Gamble Co.), and a Du Pont Young Faculty Award to M.C. and through the Defense Advanced Research Projects Agency funding to the Naval Research Laboratory.

‡ The Ohio State University.

§ Naval Research Laboratory.

[1] Abbreviations: CPK, Corey–Pauling space-filling atomic models with Koltun connectors; d_{b-b}, the distance between the glycerol backbones measured across the hydrocarbon region; $DC_{8,9}PC$, 1,2-ditricosa-10,12-diynoyl-*sn*-glycero-3-phosphocholine; d_L, lipid layer thickness; DMPE, 1,2-dimyristoyl-*sn*-glycero-3-phosphoethanolamine; d_{pol}, the distance between the phosphate-containing headgroups measured across the intervening water region; d_{p-p}, the distance between the phosphate-containing headgroups measured across the hydrocarbon chain region; DPPC, 1,2-dipalmitoyl-*sn*-glycero-3-phosphocholine; DPPG, 1,2-dipalmitoyl-*sn*-glycero-3-phosphoglycerol; DSC, differential scanning calorimetry; DTPC, 1,2-ditricosanoyl-*sn*-glycero-3-phosphocholine; d_W, water layer thickness; d_{00l}, lamellar repeat spacing; $F(00l)$, the structure factor for the $00l$ reflection; H_{II}, inverted hexagonal phase [the lipid phase notation used is that of Luzzati (1968)]; L_α, lamellar liquid crystal phase; $L_{\beta'}$, lamellar gel phase; L_C, lamellar crystalline phase; P_δ, two-dimensional centered rectangular phase with chains in the δ conformation; PLM, polarizing light microscopy; MLV, multilamellar vesicles; R, resolution of the electron density profile; R_α, primitive rectangular lattice; RH, relative humidity; $s = 2 \sin \theta/\lambda$, the reciprocal lattice coordinate; SBS, stacked bilayer sheets; SUV, small unilamellar vesicle; T_t, chain order/disorder transition temperature; $\bar{v}_L$, partial specific volume of the lipid. Lipid notation used is as follows. The lipid is named according to the position of the triple bond rather than the number of carbon atoms in the fatty acyl chain. In the case of $DC_{8,9}PC$, the first subscript, 8, indicates that there are eight methylene units between the carboxyl carbon at position 1 and the acetylene carbon at position 10 on the acyl chain. This is known as the *n*-segment of the hydrocarbon chain. The second subscript, 9, indicates that there are nine methylene units between the acetylene carbon at position 12 and the terminal methyl group and is known as the *m*-segment of the hydrocarbon chain.

0006-2960/91/0430-2134$02.50/0

al., 1987; Burke et al., 1988; Rosenblatt et al., 1987). Tubular microstructures of $DC_{8,9}PC$ can be formed in two ways. The first involves isothermal precipitation from ethanol/water mixtures (Georger et al., 1987). This method results in the formation of tubules (and helices) with an average length of 150–300 μm and diameter of 0.5–1.0 μm. The walls of the tubules can vary from 1 to ca. 10 bilayer sheets stacked one atop the other (Georger et al., 1987). The second method requires cooling an aqueous suspension of large multilamellar vesicles (MLV) through the chain order/disorder transition (T_t) (Yager & Schoen, 1984). This "thermal" method of tubule formation is dependent on the curvature of the fluid phase morphology, as small unilamellar vesicles (SUV) do not form tubules upon cooling through T_t (Rudolph & Burke, 1987; Burke et al., 1986, 1988). Instead, SUVs will supercool to 2 °C, where an exothermic event is observed that correlates with the formation of large domains of flat bilayers or stacked bilayer sheets (SBS) (Rudolph & Burke, 1987; Burke et al., 1986, 1988; Rudolph et al., 1987). Interestingly, tubules can be formed from SBS by heating and subsequent slow cooling through T_t. The tubules formed by the thermal methods are shorter (30–60 μm) than those formed by isothermal precipitation. However, quantitative measurements of the length/diameter distributions of tubules formed by the various methods have not been reported.

Although the tubules formed by isothermal precipitation from ethanol/water mixtures are morphologically similar to those obtained by cooling an aqueous suspension of MLV, little data exist as to whether the tubules formed by these two methods are similar at the nanostructure level. The first small-angle X-ray diffraction data reported on the diacetylenic lipids revealed a very small unit cell size for the isothermally prepared tubules of $DC_{8,9}PC$ (Rhodes et al., 1988). The corresponding one-dimensional electron density profile was interpreted in terms of a combination of chain tilting and partial chain interdigitation.

The majority of the physicochemical data on $DC_{8,9}PC$ tubules have been obtained with thermally formed microstructures. Infrared and Raman spectroscopic studies indicate that the acyl chains of $DC_{8,9}PC$ tubular microstructures (formed by cooling MLVs) are highly ordered and exhibit very tight chain packing (Yager & Schoen, 1984; Rudolph & Burke, 1987; Schoen et al., 1987; Sheridan, 1988). This is evidenced by the appearance of longitudinal acoustic modes of the acyl chains in the low-frequency region of the Raman spectra (Schoen & Yager, 1985; Rhodes et al., 1987). In addition, the strong wagging and rocking CH_2 modes in the infrared spectra are again indicative of acyl chains with a high degree of conformational order and many all-trans segments (Rudolph et al., 1987b; Snyder et al., 1978).

We have used low- and wide-angle X-ray powder diffraction to look for differences in long- and short-range order in the two fully hydrated, low-temperature morphologies of $DC_{8,9}PC$ formed by thermotropic methods. The X-ray data indicate that SBS and tubules have *identical* hydrocarbon chain packing in the bilayer. Furthermore, this tight packing arrangement is insensitive to the degree of hydration of the lipid, as similar X-ray patterns are observed in the dry powder and in the fully hydrated tubule and SBS low-temperature phase. This result is supported by calorimetric data, which reveal a similar T_t upon cooling the dry powder and the hydrated tubules. By applying X-ray diffraction analysis to oriented samples, high-resolution, one-dimensional electron density profiles across the bilayer repeat unit of the low-temperature morphologies have been obtained. On the basis of these data a model is proposed for the packing of individual lipid molecules in the bilayer that is consistent with the X-ray data, that is likely to facilitate polymerization, and that seems reasonable on energetic grounds. In addition, the effect of different methods of tubule preparation on their structural properties is reported.

Experimental Procedures

Materials. $DC_{8,9}PC$ was obtained as a gift from Dr. Alok Singh. The purity of the lipid was determined by thin-layer chromatography and yielded a single spot on silica gel 60 F-254 (E. Merck) by using a chloroform/methanol/water (65:25:4 by volume) solvent system with sample loading of approximately 0.1 mg of lipid in 30 μL of solvent. The saturated analogue of $DC_{8,9}PC$, DTPC, was obtained from Avanti Polar Lipids (Birmingham, AL) and was used without further purification.

Calorimetry. Aliquots of DTPC and $DC_{8,9}PC$ were dried from chloroform by heating at 60 °C under a stream of dry nitrogen and placed in a vacuum desiccator for 48 h to remove all traces of solvent. The samples were lyophilized for 48 h to remove residual water. Following lyophilization, samples were opened in a drybox purged with dry nitrogen and 2–5 mg was loaded into and sealed in stainless steel DSC pans previously stored in the vacuum desiccator. Lipid weights were determined from the known weight of the pan before and after introduction of the sample. A Perkin-Elmer DSC-7 (Perkin-Elmer Corp., Norwalk, CT) was used to collect the calorimetric data. Samples were cycled at 1 °C/min until successive scans were repeatable. Following this same sample preparation procedure, a transition temperature of 82 °C was obtained for dipalmitoylphosphatidylcholine (DPPC). This is in good agreement with value obtained by Chapman et al. (1967) for the DPPC dihydrate. Hydrated samples were prepared for calorimetry and X-ray diffraction as previously described (Rudolph & Burke, 1987).

X-ray Diffraction. Powder Samples. Samples for X-ray diffraction were prepared by loading an 80 mg/mL suspension of SUVs at 50 °C into preheated capillaries. The capillaries were cooled in a water bath to 0 °C and held for 30 min. Previous studies have shown that this results in the complete conversion of SUVs to the SBS low-temperature phase (Rudolph & Burke, 1987; Burke et al., 1986). Some capillaries were removed at this point for X-ray measurement. The remaining capillaries were heated to 50 °C and then cooled to 25 °C to form tubules. Periodically, at the end of the cycle, capillaries were opened and examined under the optical microscope to confirm the presence of tubules. Dry samples were prepared for X-ray measurement by lyophilizing the lipid previously dried from chloroform. These samples were then opened in a glovebox purged with dry nitrogen and capillaries were loaded with 2–5 mg of lipid.

X-ray powder diffraction measurements were made with wiggler-enhanced synchrotron radiation on the A1 line at the Cornell High Energy Synchrotron Source (CHESS). The experimental arrangement and precautions implemented to minimize X-radiation damage have been previously described (Caffrey, 1984). Diffraction patterns were recorded on X-ray-sensitive film (DEF-5, Kodak, Rochester, NY) and temperature was controlled to ±1.5 °C by using a forced-air crystal heating/cooling apparatus. The air stream was coaxial with the sample capillary. Exposure times varied from 10 s to 3 min depending on the beam current, sample-to-film distance, sample composition, and mesomorph type. X-ray wavelength (1.57 Å) was determined by using a lead nitrate standard and a carefully measured sample-to-film distance.

Oriented Samples. $DC_{8,9}PC$. Oriented samples were prepared for X-ray diffraction mesurement in two different ways depending on the method employed for the formation of tubules. For tubules prepared via SUVs (described above), a modification of the technique described by Rhodes et al. (1988) was employed. Approximately 0.25 mL of the concentrated tubule suspension (80 mg/mL) was dispersed on a glass slide with a Pasteur pipette. Since the suspension was quite viscous it was possible to position the slide vertically in a fixed-angle centrifuge (Model MR 14.11, Jouan, Winchester, VA). To prevent the suspension from running off the edges of the slide during centrifugation, a shield of aluminum foil was placed around the slide. The sample was then centrifuged at 2500 rpm for approximately 25 min at room temperature (22 °C). This method produced a transparent film, suggesting that a well-aligned sample had been prepared. The high degree of orientation and lack of damage to the tubules was verified by using polarizing light microscopy (PLM). The film was then incubated in the dark in an atmosphere equilibrated with different saturated salt solutions (O'Brien, 1948) for at least 20 h at 22 °C. This method produced highly oriented samples as evidenced by the fact that chain packing reflections were not observed in standard one-dimensional, θ–2θ diffraction scans. To verify that the phases investigated with oriented and powder samples were the same, another film was prepared exactly as above for an aligned sample, but with the lipid centrifuged onto a roughened glass slide. This sample generated a powder diffraction pattern such that several chain packing reflections were observed in the θ–2θ scans that coincided with those seen by the powder method.

To compare the effects that different tubule preparation methods have on the structural characteristics of the resulting tubules, samples were also prepared via precipitation from an organic solvent. This is the method first proposed by Georger et al. (1987). By varying organic solvent identity, solvent/water ratio, and incubation time after tubule formation, it is possible to adjust the length of the tubules and to produce more open, helical structures. In this work an adaptation of the Georger et al. isothermal precipitation method was used. One milligram of $DC_{8,9}PC$ was dissolved in 0.7 mL of absolute ethanol and incubated at 50 °C for 45 min. Water (also at 50 °C) was then added so that the final solvent composition was ethanol/water (70/30, v/v) and the lipid concentration was 1 mg/mL. The solution, contained in a test tube, was cooled at 0.2 °C/min in a water bath (Neslab RTE-210 with a MTP-6 programmer, Neslab, Newington, NH) through the thermotropic phase transition (approximately 30 °C in this solvent system) to a final temperature of 20 °C. A range of cooling rates was employed and it was found that the slower the rate, down to 0.2 °C/min, the longer the tubules. This method produced tubules measuring 0.15 mm. If the tubules were incubated at ca. 20 °C in the suspending ethanol/water solution, they grew longer with time, and after 4 days some were over 0.18 mm in length and had started to bend about the long axis of the tubule. Helical structures were not observed at any time.

To produce an aligned sample prepared via the isothermal method the tubules were pelleted in a swinging-bucket centrifuge (IEC 428, Baxter Healthcare Corporation, IL), for approximately 25 min, and the concentrated suspension was dispersed on a glass slide. The solvent was allowed to evaporate slowly in a humid atmosphere of saturated NaBr solution (57% RH), in the dark, at room temperature for at least 3 days. Again the sample was examined by PLM to verify that the tubules had remained intact.

DTPC. When the saturated analogue, DTPC, was subjected to the same treatment as $DC_{8,9}PC$ in the isothermal method, a texture indicative of a lamellar phase was observed by PLM. The presence of tubules was not detected. The method that produced the most oriented sample (as judged by the absence of diffraction arising from the chain packing in the θ–2θ scans) was to first dissolve approximately 20 mg of the lipid in about 0.2 mL of an ethanol/water mixture (80/20 v/v). All of the solution was then placed on a glass slide and left in an atmosphere of 100% RH at ca. 85 °C, i.e., 6 °C above the main chain "melting" transition temperature of 79 °C (Burke et al., 1988b), for approximately 2 h. The entire humidity chamber was then allowed to cool passively to room temperature at the rate of ca. 10 °C/h by leaving the chamber in the oven after shutting off the power. The sample was then incubated at 57% RH and 22 °C for at least 48 h.

A Rigaku, Geigerflex camera with D/MAX-B system software (Danvers, MA) was used to collect θ–2θ diffraction scans on oriented samples. The X-ray tube was operated at 40 kV and 30 mA and Cu $K\alpha_1$ radiation at 1.5405 Å was used. θ–2θ scans were recorded from 0.8° to 25–35° in steps of 0.05° at a rate of 5 deg/min. Complete diffraction patterns were collected in about 10 min.

To prevent extensive polymerization of the diacetylenic lipid in the X-ray beam, a new portion of the sample was exposed for each diffraction measurement. Thus, no one part of the sample was exposed to the X-ray beam for more than 10 min. Under these conditions, no color developed in the lipid during a typical exposure.

Electron Density Profile Determination. To decipher the conformation of the $DC_{8,9}PC$ and DTPC lipid molecules in their respective morphologies, the diffracted intensity distribution in the θ–2θ scans were analyzed to yield one-dimensional electron density profiles. Integrated peak intensity was calculated by paper weighing. Background scatter was removed by subtracting a baseline drawn connecting either side of the diffraction peak. The background-corrected integrated intensity values [$I(00l)$] were also corrected for geometric factors (the Lorentz correction) so that the modulus value of the structure factor amplitude of the ($00l$) order, $|F(00l)|$, was set equal to $[(00l)\cdot I(00l)]^{1/2}$. The changes in $|F(00l)|$ as the RH and, therefore, the lamellar repeat spacing increased were plotted as a function of the reciprocal space coordinate, s (where $s = 2 \sin \theta/\lambda$). This so-called swelling method provides the continuous transform for the unit cell from which the phase angles for the various structure factor amplitudes can be determined. At each RH, the structure factor amplitudes were normalized according to the procedure of Blaurock (1967). The nodes at which the phase angle changes occur are suggested by amplitude data alone and have been confirmed by the Shannon sampling theorem method (Shannon, 1949; Sayre, 1952; Franks & Levine, 1981; McIntosh & Simon, 1986). Electron density profiles were constructed by using standard Fourier synthesis methods (Franks & Levine, 1981; Kim et al., 1987; Franks, 1976; McIntosh et al., 1983). As cosine terms of higher frequency are added to the synthesis, i.e., as l increases, finer detail can be resolved in the electron density profile. The resolution R, therefore, depends on the highest angle at which diffraction is recorded. For the lamellar phase that is periodic in one-dimension, R is given by (d/l_{max}), where l_{max} is the highest diffraction order observed. For the high-resolution profiles ($l = 15$), phase angle assignments were made by using the swelling series to the limit of its sampling of reciprocal space (typically $l = 10$). The higher order terms were phased by using a pattern recognition technique (Luzzati

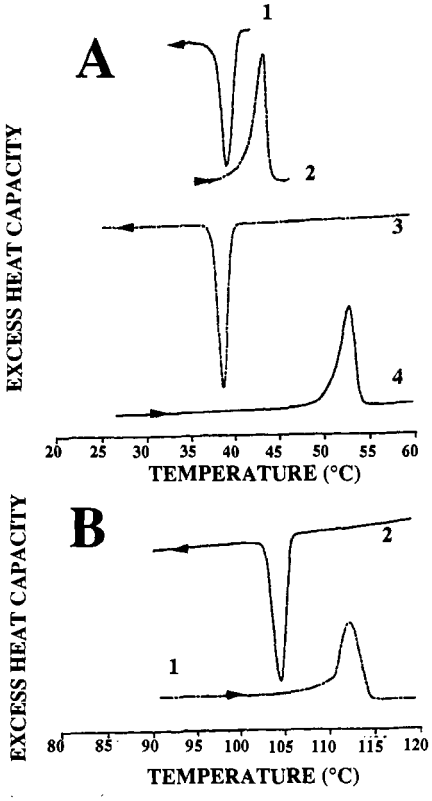

FIGURE 1: Differential scanning calorimetry of $DC_{8,9}PC$ and its saturated analogue DTPC. The heating (4) and cooling (3) scans for dry $DC_{8,9}PC$ are shown in panel A and heating (1) and cooling (2) scans for dry DTPC in panel B. For ease of comparison we have included in panel A the heating (2) and cooling (1) scans for fully hydrated $DC_{8,9}PC$. Scan 1 in panel A corresponds to the transformation from sheets to tubules. All measurements were made at a rate of 1 °C/min.

et al., 1972). The criterion used for correct assignment was the phase sequence, giving the flattest electron density profile in the methylene segment regions of the bilayer interior.

Partial Specific Volumes. A neutral bouyancy technique was used to determine partial specific volumes for each lipid in its different morphologies. For $DC_{8,9}PC$ both the tubule and MLV forms were examined. For DTPC, gel phase MLVs alone were studied. Samples of lipid were dispersed in a range of H_2O/D_2O mixtures and sealed in small test tubes. For the MLV samples, the suspension was heated to approximately 10 °C above the main chain melting transition (T_t = 38 °C for $DC_{8,9}PC$ and 79 °C for DTPC), then vortexed, and allowed to cool to room temperature. This procedure was repeated several times. Tubules obtained via the SUV method in H_2O were simply dispersed in a vast excess of the appropriate H_2O/D_2O mixture. The lipid was allowed to equilibrate in a temperature-regulated room (T = 21 °C) for up to 6 days. The partial specific volume of the lipid, $\bar{v}_L$, was determined from the H_2O/D_2O mixture, giving neutral bouyancy with an estimated accuracy of 2 μL/g.

RESULTS

Calorimetry. The DSC scans for dry $DC_{8,9}PC$ are presented in Figure 1. For comparison, data obtained with the fully hydrated lipid illustrating tubule formation from SBS are also included (Yager & Schoen, 1985; Rudolph & Burke, 1987; Burke et al., 1986; Rudolph et al., 1987). The dry lipid shows an endotherm at 52.7 °C (onset = 50.6 °C) with an enthalpy of 22.9 kcal/mol. Cooling results in an exotherm at 38.6 °C (onset = 40.4 °C) with an enthalpy of −22.5 kcal/mol. The corresponding values for the heating and cooling of hydrated lipid are respectively T_t = 42.6 and 39.7 °C and ΔH = 24 kcal/mol and are in agreement with previously published data (Yager & Schoen, 1985; Rudolph & Burke, 1987).

Figure 1B shows the calorimetric scans for the dry saturated analogue, DTPC. Upon heating an endotherm is observed at 112 °C (onset = 110.3 °C) with an enthalpy of 12.4 kcal/mol. Subsequent cooling results in an exotherm at 104.5 °C (onset = 105.7 °C) with an enthalpy of −12.3 kcal/mol. While the enthalpies are similar, the width of the transition is considerably larger in the heating direction.

X-ray Diffraction. Powder Samples. $DC_{8,9}PC$ Tubules. As a structural complement to the DSC and earlier FTIR measurements, static low- and wide-angle X-ray diffraction measurements were performed on fully hydrated $DC_{8,9}PC$ tubules prepared in a manner identical with that used for calorimetric scans. Patterns were recorded on X-ray-sensitive film at a series of temperatures above (44, 48 °C) and below (27, 35, 40 °C) the chain melting transition determined by DSC in both the heating and the cooling directions. Sample patterns are shown in Figure 2 and the corresponding d spacings and phase designations are presented in Table I.

In the low-angle region below T_t, four lines are apparent, which index on a one-dimensional lamellar lattice with d_{00l} = 66.4 Å. The reflections have significant breadth and occasionally show an arched intensity distribution, suggesting a preferential orientation of the lamellae in the X-ray capillary (Figure 2A). The intensity in each reflection as a function of order (l) is as follows: strong (l = 1), strong (l = 2), weak (l = 3), strong (l = 4). The wide-angle region is dominated by a series of sharp and broad reflections visible out to 4 Å (Table I and Figure 2). The area beyond this the pattern is dominated by the diffuse water peak centered at ~3.3 Å. At intermediate angles a line at 10.2 Å and possibly a second at 9.57 Å, which is only noticeable on the more heavily exposed films in a pack, is visible. This phase is designated the lamellar crystalline (L_c) phase.

This pattern persists unchanged in lattice type and parameters up to 40 °C. At 44 °C, a completely different pattern is observed, which is characteristic of the lamellar liquid crystalline (L_α) phase. In this case, two sharp reflections at 73 and 36 Å are present in the low-angle region accompanied by a diffuse ring centered at ca. 4.5 Å. The latter is characteristic of a lamellar phase with d_{00l} = 72.5 Å and with a "fluidlike" hydrocarbon compartment. The tubule morphology is lost upon heating into the L_α phase. The L_α pattern persists up to 48 °C (Table I).

Upon cooling from the L_α phase to 27 °C, the L_c phase, with a slightly larger lamellar repeat, is restored, indicating the reversibility of the transition in terms of both mesomorph type and chain packing lattice parameters. A possible undercooling phenomenon was not examined for in these experiments. These data show that the transition observed by DSC and FTIR is of the L_c/L_α type.

$DC_{8,9}PC$ Stacked Bilayer Sheets. Diffraction measurements were performed on fully hydrated sheets of $DC_{8,9}PC$ as indicated above at 27, 35, 39, 40, 42, and 48 °C in the heating direction (SBS morphology) and at 27 °C upon cooling (tubular morphology). Essentially identical results were obtained with sheets as with tubules with regard to transition temperature and reversibility, lattice type, symmetry, and lattice parameters both above and below the L_c/L_α transition. A slight difference was noted in the lamellar repeat size in the L_α phase. However, this is not considered significant since only two orders were recorded in either case. These data are presented in Table I and support the FTIR data, which indicated little difference if any in the structural features of

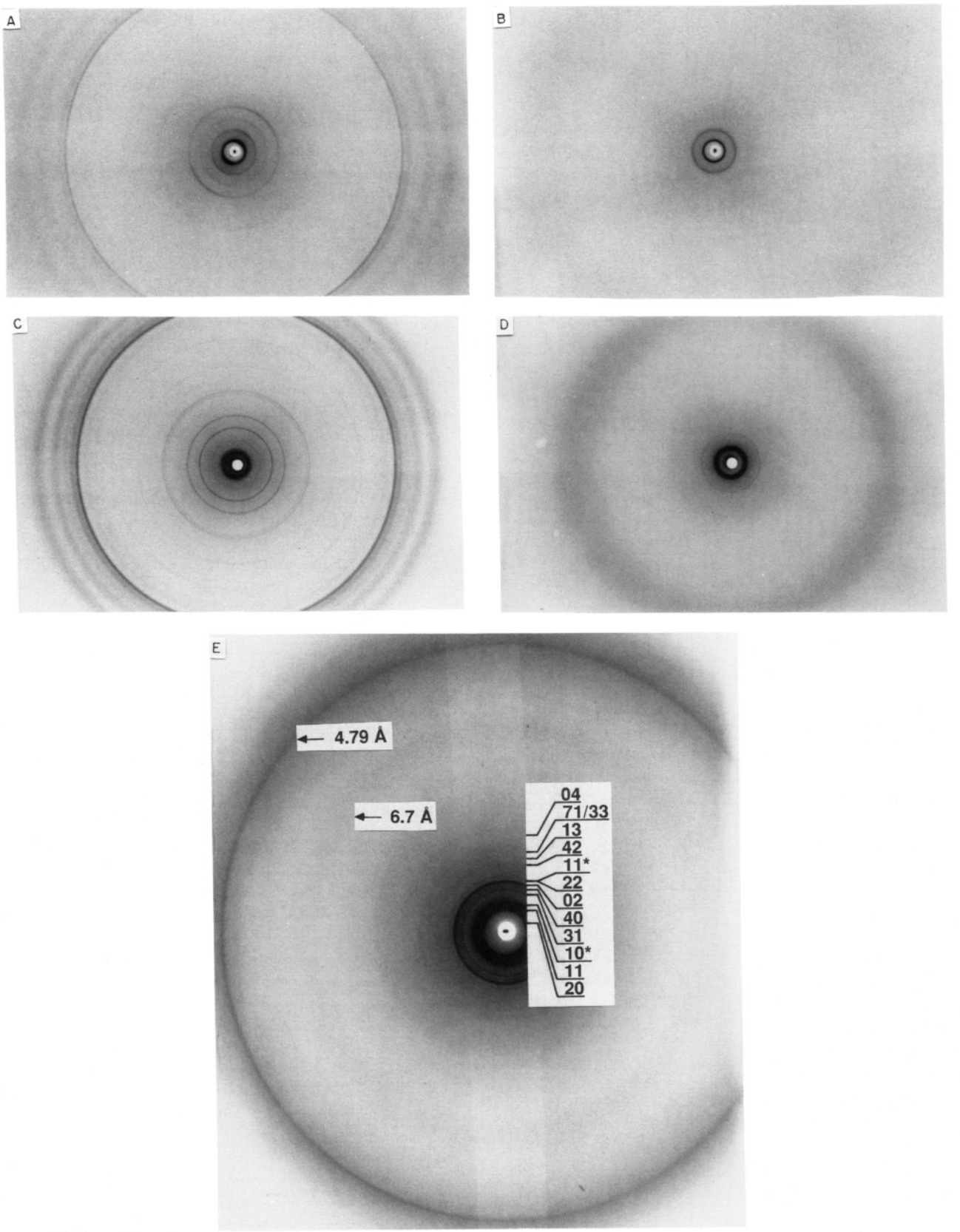

FIGURE 2: X-ray diffraction patterns of $DC_{8,9}PC$ and DTPC under dry and fully hydrated conditions. $DC_{8,9}PC$ as fully hydrated tubules in the L_c phase at 27 °C (A) and in the L_α phase at 46 °C (B). Dry $DC_{8,9}PC$ in the L_c phase at 39 °C (C) and in the R_α/L_α phase coexistence region at 55 °C (D). Dry DTPC in the P_δ/H_{II} phase coexistence region at 112 °C (E). The P_δ and H_{II} (denoted by an asterisk) Miller indices are included along with the *d* spacing of the onset of diffuse scatter at 6.7 Å and the sharp reflection at 4.79 Å. Patterns were recorded as described under Experimental Procedures, with sample-to-film distances ranging from 5 to 10 cm.

tubule and sheet microstructures of fully hydrated $DC_{8,9}PC$ (Rudolph & Burke, 1987).

Dry $DC_{8,9}PC$. Given that the calorimetric behavior of fully hydrated $DC_{8,9}PC$ tubules and of dry $DC_{8,9}PC$ is similar, particularly in the cooling direction, complementary X-ray diffraction measurements were made on the dry powder both above and below T_t to determine if such thermotropic similarities had a structural analogue. Measurements were made

Table I: X-ray Diffraction Data and Phase Designation for Hydrated $DC_{8,9}PC$ Sheets and Tubules and for the Dry Powder of $DC_{8,9}PC$ and Its Saturated Analogue DTPC

	hydrated $DC_{8,9}PC$						dry powder					
	tubules[d]			sheets			$DC_{8,9}PC$[d]			DTPC[h]		
	27 °C	48 °C	↓27 °C	27 °C	48 °C	↓27 °C	39 °C	55 °C	↓27 °C	19 °C	112 °C	↓29 °C
lamellar repeat (Å)[a]	66.4 (4)	73.1 (2)	68.3 (4)	66.4 (4)	74.2 (2)	68.0 (4)	57.6 (8)	55.6 [10] 41.7 [01] 33.4 [11] 27.8 [20] 23.2 [21][i] 15.6 [003]* 12.4 [23]	57.8 (11)	78.3M 63.4S 32.8M 29.1M 21.6M 20.2M	56.0 [20] 47.1 [11] 41.0 [10]* 30.7 [31] 27.7 [40] 25.7 [02] 23.7 [22]	68.3 (10)
wide-angle scattering (Å)	10.2W[c] 9.57W 7.50W 5.21W 4.93W 4.64S 4.49M 4.08W		4.60S 4.48M 4.07W 3.77W	10.1W 9.65W 7.24W 5.18W 4.91W 4.60S 4.49M 4.30W 4.08M 3.74M		9.79W	10.02W 9.65W[f] 8.24W 7.24W 5.77W 5.15W 4.84W 4.59S 4.45M 4.29W 4.07W 3.76M 3.41M 2.80W	11.7 [004]*	9.91W 9.65M 8.24W 7.24M 5.78W 5.26W 4.83W 4.59S 4.46M 4.28W 4.06M 3.74M 3.39W 2.80W	4.99W 4.64W 4.37M 4.19M 4.03W 3.90W 3.83W	23.7 [11]* 19.1 [42] 17.4 [13] 15.5 [33] 15.5 [71] 12.9 [04] D6.7W D4.8S 4.78S	8.57W 6.82W 6.52W 5.69W 5.26W 4.89W 4.66M 4.24S 4.09M[g]
	D3.30S[b]	D4.4W[e] D3.27S	D3.30S	D3.23S	D4.7W[e] D3.27S			D4.5S				
phase designation	L_c	L_α	L_c	L_c	L_α	L_c	L_c	R_α,[j] *L_α[k]	L_c	C_o	P_δ,[l] *H_{II}[m]	L_{CI}

[a] Lamellar repeat distance has an error of ±1 Å due to difficulties in determining peak positions on very strong peaks and a low number of orders. Values are reported to one decimal place as a result of averaging over orders. Number of orders recorded are given in parentheses. Wide- and intermediate-angle lines are good to better than ±0.1 Å. [b] D denotes that the peak was diffuse; all others are sharp. [c] Intensity ratings are S, strong; M, medium; and W, weak. [d] Measurements made upon sample cooling are indicated by ↓. [e] The disordered chain scattering peak was so weak as to preclude accurate peak position determination. [f] Underlined reflections index as higher orders of the (001) line listed in the low-angle region. [g] This constitutes a broad shoulder on the wide-angle side of the strong sharp peak at 4.24 Å. [h] Because of the complex nature of the low-angle pattern for DTPC at the 19 and 112 °C pattern, all of the lines in this region are reported. [i] Could also index as the [002] reflection of the lamellar lattice. [j] The corresponding lattice parameters are a = 55.6 Å and b = 41.7 Å. The calculated d-spacing values for the R_α phase are 55.6 Å [10], 41.7 Å [01], 33.4 Å [11], 27.8 Å [20], 23.1 Å [21], 15.6 Å [003], 12.4 Å [23], and 11.7 Å [004]. Values are calculated according to the equation $s^2_{hk} = h^2a^{*2} + k^2b^{*2}$, where a^* and b^* are dimensions of the reciprocal unit cell (Luzzati, 1968). [k] The corresponding lattice parameter is d_{001} = 46.8 Å. [l] The corresponding lattice parameters are a = 111.4 Å and b = 51.9 Å. The calculated d-spacing values for the P_δ phase are 55.7 Å [20], 46.9 Å [11], 30.1 Å [31], 27.9 Å [40], 25.8 Å [02], 23.4 Å [22], 18.9 Å [42], 17.0 Å [13], 15.6 Å [33], 15.2 Å [71], and 12.9 Å [04]. Values are calculated according to the equation $s^2_{hk} = h^2a^{*2} + k^2b^{*2}$, where a^* and b^* are dimensions of the reciprocal unit cell and $h + k = 2n$ (Luzzati, 1968). [m] The corresponding lattice parameters are d = 41.0 Å and a = 47.3 Å.

at 39, 50, and 55 °C upon heating and at 42, 36, and 27 °C upon cooling. Lattice parameters for the dry material are presented in Table I and sample diffraction patterns are included in Figure 2.

At the outset we note that the patterns recorded at low temperatures were obtained by using samples that had not been previously heated. At 27 °C multiple reflections, out to l = 11, were observed that indexed on a lamellar lattice with d_{00l} = 57.6 Å. At intermediate angles the pattern reveals a sharp line at 10.2 Å. The wide-angle region is dominated by a series of sharp and broad rings out to 2.8 Å. Conspicuous by its absence, compared to the fully hydrated samples, is the diffuse water peak at 3.3 Å, which probably accounts for the appearance of a range of weaker lines in this region of the pattern. This phase is identified also as being of the L_c type.

From an examination of the wide-angle data in Table I for sheets, tubules, and dry powder at low temperatures, it is apparent that an identical chain packing conformation obtains regardless of the state of hydration and/or microscopic morphology, i.e., sheets versus tubules. However, there is a very definite effect of hydration on the measured lamellar repeat. For example, under conditions of full hydration, d_{00l} = 66.4 Å for both sheets and tubules in the L_c phase at 27 °C. In the case of the dry powder, the corresponding value is 57.8 Å. Given that chain packing is independent of hydration, we can safely assume that the increase in lamellar d spacing in the presence of excess water is solely due to an imbibition of water between the lamellae without significant alteration in the short-range order of the lipid component. In this regard, it is interesting to note that FTIR spectroscopic signatures of the C=O and P=O groups show little effect of hydration on headgroup motional characteristics (A. S. Rudolph, unpublished data).

At and above 50 °C, the dry powder appears to exhibit phase coexistence. At 50 °C coexisting phases can be indexed on an oblique lattice with a = 55.4 Å, b = 41.7 Å, and γ = 85.4° and a lamellar lattice (L_α phase) with d_{00l} = 46.8 Å. The angle of the oblique lattice increases with temperature, resulting in coexistence between a primitive rectangular lattice, R_α (a = 55.6 Å and b = 41.7 Å), and an L_α phase (d_{00l} = 46.8 Å) (Table I and Figure 2D). Regardless of temperature, the lamellar repeat distance is quite different from that observed under conditions of full hydration (d_{00l} = 73–74 Å), although in both cases a diffuse band centered at ca. 4.5 Å is observed, suggesting a similar state of short-range disorder in the hydrocarbon region. Upon cooling from 55 °C, the original L_c

phase is restored at 27 °C, as was observed for both hydrated sheets and tubules of $DC_{8,9}PC$, the only difference being in the size of the lamellar repeat.

It is interesting to note that by using X-ray diffraction as a means for following the chain order/disorder transition, the conversion to the L_α phase was complete by 50 °C in the case of the dry $DC_{8,9}PC$ powder. The corresponding transition temperature determined by DSC is ca. 53–55 °C. The origin of this disparate behavior is not known but may be accounted by differences in lipid hydration, sample heating protocols, and/or temperature calibration.

Dry DTPC. In addition to examining the thermotropic mesomorphism of dry $DC_{8,9}PC$, a comparison was made with the behavior of the dry, saturated analogue of the polymerizable lipid. DTPC contains two tricosanoic acids (C_{23}) in ester linkage at the *sn*-1 and *sn*-2 positions of α-glycerophosphocholine. Diffraction patterns were recorded at a series of temperatures in the range 19–133 °C and upon cooling to 29 °C. Low- and wide-angle spacings along with phase identification are shown in Table I. Diffraction patterns were recorded by using a sample that had not been previously heated and thus the data correspond to a first heating. At 19 °C, the wide-angle pattern is dominated by a series of strong and sharp reflections out to 3.83 Å. At low angles a rather complex pattern is observed. An examination of the *d* spacings in this region suggests that the sample consists of a number of phases. This may indicate the presence of different (1) hydrates as a result of incomplete drying and/or (2) crystalline polymorphs. As sample temperature was raised to 88 °C the pattern changed dramatically. It appears that at this temperature the sample consisted of at least two lamellar crystalline phases with d_{00l} = 69 and 62 Å. From 106 to 133 °C complex diffraction patterns are observed. At 112 °C, the diffraction pattern in the wide-angle region consists of a sharp reflection at 4.79 Å superimposed on a structured, diffuse scattering peak with a sharp onset at 6.7 Å (Figure 2E). This type of diffraction is typical of phases having hydrocarbon chains in the δ conformation (Tardieu et al., 1973). Such phases have stiff, helical hydrocarbon chains that are packed on a two-dimensional square lattice. The polar headgroups are oriented perpendicular to the bilayer and interdigitate with the headgroups on the apposed monolayer. The headgroups themselves are also on a square lattice, the length of which is the diagonal of the square-chain lattice. At 112 °C, 11 nonlamellar reflections were observed in the diffraction pattern of dry DTPC, which index as two distinct two-dimensional lattices (Table I, Figure 2E). Nine of these reflections index unambiguously on a centered rectangular lattice with unit cell dimensions of a = 111.4 Å and b = 51.9 Å. These data, combined with the wide-angle data presented above, are indicative of a P_δ phase. Of the two remaining reflections one is consistent with an hexagonal lattice, presumably of the inverted (H_{II}) type where d = 41.0 Å and a = 47.3 Å, while the other could be either the (11) reflection of the H_{II} phase or the (22) reflection of the P_δ phase. At 125 °C, three reflections are observed for the P_δ phase (a = 101.9 Å, b = 50.4 Å) and four for the H_{II} phase (d = 40.5 Å, a = 46.8 Å). Phase coexistence for a one-component system conflicts with the Gibbs phase rule; however, several explanations are possible including incomplete drying of the lipid as mentioned previously and phase metastability. Cooling the sample to 29 °C generates a single lamellar crystalline phase with d_{00l} = 68.3 Å. It is characterized by multiple sharp and broad rings in the intermediate- and wide-angle region of the diffraction pattern (Table I). Since this phase was obtained by a relatively rapid cooling of the partially "melted" sample, it is likely that it represents a metastable phase and that, with time, it would convert to one or other of the polymorphs observed in the sample upon first heating. A more detailed examination of this proposed metastability was not undertaken.

X-Ray Induced Polymerization. Throughout all of the diffraction measurements on the polymerizable $DC_{8,9}PC$ lipid, an X-ray-induced color change in the material was observed, which may indicate that the X-ray beam induced polymerization of the diacetylenic groups. This is based on the development of a distinct red or orange color at the point where the X-ray beam intersected the sample. The development of color could be traced through the sample by examination with a light microscope. Where the direct beam emerged from the sample was also identifiable as a well-defined colored spot.

A change in color accompanies polymerization as described previously (Yager & Schoen, 1984; Schoen & Yager, 1985; Schoen et al., 1987; Sheridan, 1988; Singh et al., 1986), although a quantitative relationship between color development and polymerization has not been established. However, coloration does indicate that some degree of diacetylenic conjugation has occurred. As a result of the observed color development in all of these measurements, it was of concern that the recorded diffraction data may have sizeable contributions from the polymerized form of the lipid. In an attempt to minimize such an effect, the following experiment was performed. A fully hydrated tubule sample 30 mm long was prepared and the diffraction pattern was recorded in the L_c and in the L_α phase while the sample was being continuously translated in the X-ray beam. In this way, no one part of the sample was exposed to the beam for ≥1.2 s.

Following the exposure, the sample showed no visible color development. The diffraction patterns recorded in this way and those recorded with stationary samples and that changed color in the course of the measurement are essentially identical in both the low- and the wide-angle region and above and below T_t. These data indicate that the measurements made with stationary samples are reliable indicators of the nonpolymerized behavior, despite color development during data collection. In addition, the data suggest that color development may not be a reliable indicator of the degree of polymerization.

Of note also is the fact that during an X-ray exposure below the chain melting transition the color change is from white to reddish brown. In the L_α phase a white-to-orange color change is observed, which persists upon cooling to 27 °C. When a sample, previously exposed in the L_c phase, that has red coloration is warmed to above T_t, the red changes to orange, a color that persists upon cooling through T_t. The thermochromic effect with $DC_{8,9}PC$ has been documented previously (Singh et al., 1986). As judged by visual inspection, there is no diffusion of the color upon storage for extended periods (months) in the 20–30 °C temperature range. If the change in color is associated with the polymerization reaction, then these results show that X-rays are capable of inducing such polymerization at doses of $\leq 10^6$ rads (Caffrey, 1984).

Oriented Samples. θ–2θ scans of the diffracted intensity from oriented preparations of $DC_{8,9}PC$ and DTPC at 57% RH and 22 °C are shown in Figure 3. In the tubular morphology (prepared via the thermal/SUV method) $DC_{8,9}PC$ revealed a well-ordered phase with up to 15 lamellar reflections and a repeat spacing of 59.0 Å. Ten lamellar reflections were observed for the saturated analogue, DTPC. In this case the repeat spacing was 71.4 Å. On the basis of separate experiments using more powderlike samples where the wide-angle diffraction region was found to contain a peak at 4.3 Å and

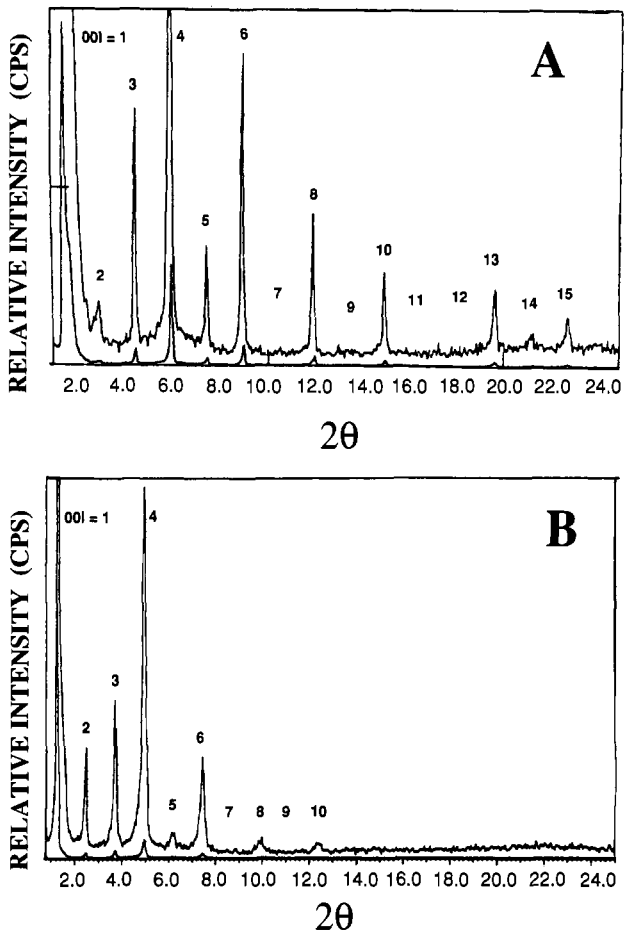

FIGURE 3: θ–2θ diffracted intensity scans of $DC_{8,9}PC$ (A) and DTPC (B) oriented samples at 57% RH and 22 °C. The L_C phase of $DC_{8,9}PC$ in tubule morphology is shown in panel A. The lamellar gel phase ($L_{\beta'}$) of DTPC is shown in panel B. Scans were recorded as described under Experimental Procedures. The lamellar repeat order number is indicated above each peak. The lamellar repeat spacing is 59.0 Å in panel A and 71.4 Å in panel B.

a broad band centered at 4.0 Å, a gel-phase assignment of the $L_{\beta'}$ (tilted chains) type was made (Tardieu et al., 1973). Upon increasing the RH in a stepwise manner for the oriented sample of the diacetylenic lipid, a swelling series was generated, and at 86% RH, the lamellar repeat spacing had increased to 65.6 Å. The normalized structure factor amplitudes ($|F_n(00l)|$) for this swelling series are shown as a function of the reciprocal lattice coordinate s in Figure 4A. The data collected in the RH range 57–86% fall on a smooth curve indicating that the unit cell, and, thus, the structure of the bilayer, did not change significantly upon hydration. The normalized structure factor amplitudes for the saturated lipid swelling series are plotted as a function of s in Figure 4B. At 100% RH, the lamellar repeat spacing had risen to 76.4 Å. The corresponding electron density profiles obtained from these swelling series data for $DC_{8,9}PC$ and DTPC will be described under Discussion.

The X-ray diffraction parameters obtained for $DC_{8,9}PC$ at 57% RH and 22 °C in tubular morphology prepared via the thermal and isothermal methods are identical (data not shown). This implies that the unit cell is the same for both. Therefore, the packing of the lipid molecules within the bilayer and the stacking of the bilayers in the tubules is the same regardless of the method used to prepare them. This indicates that ethanol may not interact with the interfacial region of the lipid in this phase and no interdigitation is observed.

Partial Specific Volumes. The partial specific volumes of $DC_{8,9}PC$ and DTPC in tubules and MLVs were determined

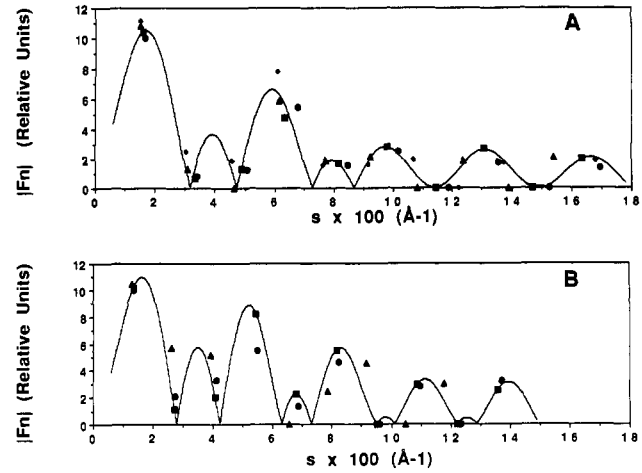

FIGURE 4: Modulus of the normalized structure factor amplitude versus reciprocal spacing for (A) $DC_{8,9}PC$ tubules and (B) DTPC in the $L_{\beta'}$ phase at 22 °C. The relative humidities used are as follows: (A) (●) 57%; (■) 63.5%; (▲) 71%; (◇) 86%. (B) (●) 57%; (■) 63.5%; (▲) 100%. The solid curves were calculated by using Shannon's sampling theorem at 63.5% RH for both $DC_{8,9}PC$ and DTPC.

by the neutral buoyancy method at 21 °C as described under Experimental Procedures. For $DC_{8,9}PC$ values of 0.923 and 0.912 mg/mL were determined for the MLV and tubule morphology, respectively. The corresponding value for DTPC in MLVs is 0.951 mg/mL. From molecular weights of 914 and 930 g/mol for $DC_{8,9}PC$ and DTPC, molecular volumes of 1407, 1390 and 1470 Å^3 have been calculated, respectively, for the diacetylenic lipid in the MLV and tubule form and for the saturated analogue as MLVs.

Discussion

Lipid Bilayer Models. A complete hydration series, wherein the water/lipid ratio is varied in a known manner up to saturation, was not performed on the powder samples used in this study. Thus, the relative contributions of water (d_w) and lipid (d_L) to the measured d spacing (d) for tubules and sheets have not been determined. In the case of the dry $DC_{8,9}PC$ and DTPC powders, however, d_w reduces to zero and the measured d equals d_L. In an initial attempt to understand the arrangement of lipid molecules in the L_c and L_α phases for both of the lipids, calculations of molecular dimensions were performed with the aid of CPK space-filling models, accepted bond distances and angles and measured d spacings.

One of the $DC_{8,9}PC$ configurations chosen for examination is shown in Figure 5. Here, the standard glycerophosphocholine configuration was used with the choline headgroup oriented approximately parallel to the bilayer surface and the glycerol backbone parallel to the all-trans methylene segments of the *sn*-1 chain (Buldt et al., 1978).

In this unstrained configuration, the molecule measures 40.0 ± 0.5 Å along its long axis. This is made up of (a) 12.4 Å for the glycerophosphocholine headgroup and includes the COO moiety of the *sn*-1 chain (b) 9.8 Å from the center of the CH_2–CO bond to the center of the C9–C10 bond on the *sn*-1 chain, (c) 4.2 Å to the center of the C13–C14 bond, and (d) 13.6 Å to the tip of the terminal methyl. There is a gap of ca. 3 Å separating the diyne moieties on adjacent chains. The diyne introduces a kink or jog in the chains causing a relative displacement of the n and m methylene segments on the same chain amounting to 3.6 Å.

With this basic configuration, a variety of molecular arrangements were considered as ways in which $DC_{8,9}PC$ molecules assemble in the L_c phase, one of which is shown in

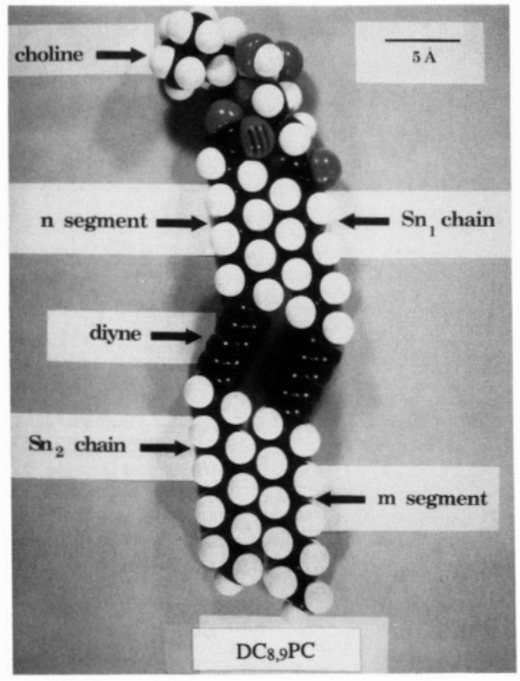

FIGURE 5: CPK space-filling molecular model of $DC_{8,9}PC$. A length scale plus identifying features of the molecule are included. In the case of $DC_{8,9}PC$ *n* and *m* correspond respectively to the methylene segments containing 8 and 9 methylene units.

Figure 6A. This particular model offers compact packing of chains and headgroups. Molecules are tilted with the long axis at a 32° angle with respect to the bilayer normal. The diyne moieties line up in close proximity to each other with their long axes approximately parallel to the bilayer normal. The major divisions within the bilayer in this model are a central terminal methyl group region, two methylene segments separated by the diyne moiety band, and an outer polar headgroup region. The model is least compact in the plane containing the diyne moieties. However, the alignment of adjacent diynes above and below the plane containing the lipid in Figure 6A is likely to facilitate polymerization. No significant chain interdigitation at the bilayer midplane is observed.

The current model presents the *m* and *n* segments of the molecule in a "trans" configuration when viewed down the long axis of the diynes (Figure 6B,C). There is free rotation about the central C–C single bond connecting the two acetylenic bonds and, indeed, about the C–C single bonds on either side of the triple bonds. Accordingly, a range of bilayer arrangements can be generated simply by rotating the *m* segment relative to a fixed *n* segment. Some extreme examples are schematically represented in Figure 6. The model shown in Figure 6A derives from the trans conformation. Attempts to construct a compact bilayer from the eclipsed conformer were unsuccessful. No matter how the molecules were arranged an open and, thus, thermodynamically unfavorable structure was obtained.

For conformations other than trans and eclipsed, the lipid molecule is no longer planar (Figure 6). Coupling of such *m* segments across the bilayer midplane and beyond would give rise to a screwlike configuration and possibly to superstructures (helices) in the dry state. We have not considered such structures in any detail.

In the dry condition, the saturated analogue, DTPC, forms a single, possibly metastable, lamellar crystalline phase (L_{C1}) upon rapid cooling from 133 °C. The lamellar repeat is 68.3 Å and the diffraction pattern has multiple sharp and broad reflections in the intermediate- and wide-angle region. On the

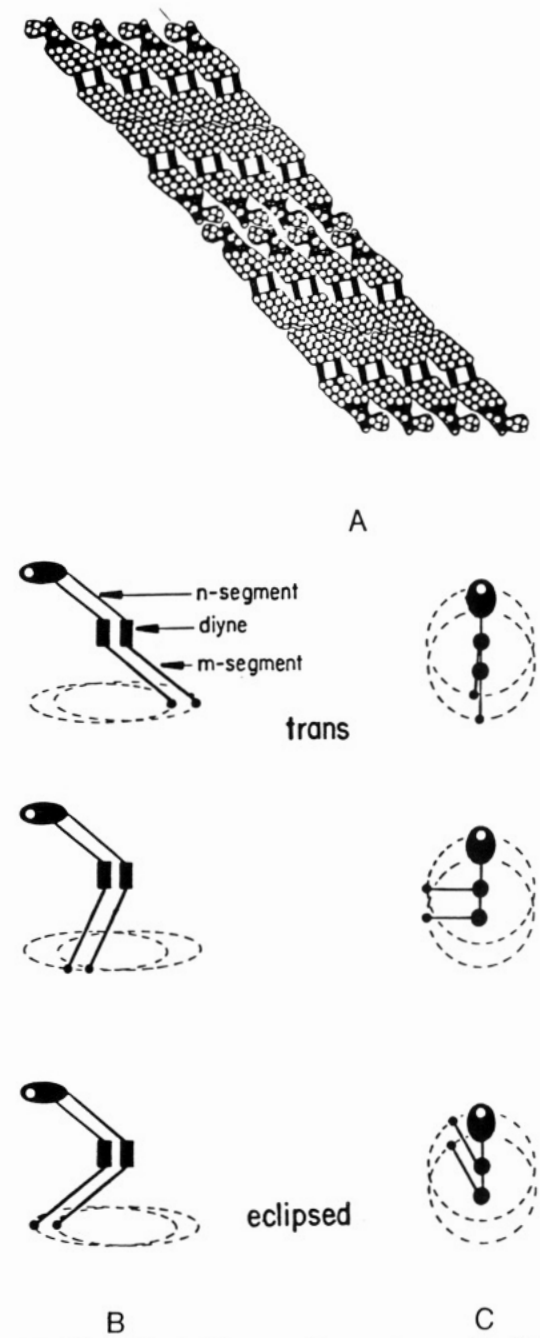

FIGURE 6: Schematic of a bilayer packing arrangement for $DC_{8,9}PC$ in the dry state providing a lamellar repeat distance of 58 Å (A). See text for details. This arrangement is made up of individual molecules with *n* and *m* segments parallel and with a fully extended all-trans conformation as shown in Figure 5. A schematic view of the $DC_{8,9}PC$ methylene segment conformations assuming free rotation about the diacetylenic moiety is shown in part B. An alternate perspective is presented in part C, where the relative positions of the *n* and *m* segments are viewed as projecting from and rotating about the diacetylenic moieties in the spirit of the Newman projection.

basis of CPK space-filling models of DTPC with the glycerophosphocholine conformation noted above and with chains in the all-trans configuration, a maximum molecular length of ca. 41 Å was measured. The terminal methyl groups on the two chains are out of register by ca. 2 Å. Allowing for interdigitation of chains to this extent at the bilayer midplane provides a bilayer thickness of 80 Å with chains parallel to the bilayer normal. Tilting the long axis of the lipid molecule by 31° from the bilayer normal is required to reduce bilayer thickness to the measured value of 68.3 Å. Interestingly, the L_{C1} diffraction pattern contains a sharp reflection at 4.24 Å

and a broad shoulder centered at 4.09 Å, reminiscent of the $L_{\beta'}$ phase in the hydrated, shorter chain PC homologues. In the case of the L_{C_1}, however, a number of additional sharp reflections at intermediate and wide angles are present, which render subcell determination problematic.

It has been noted that the high degree of order in the tubule and sheet microstructures of $DC_{8,9}PC$ was akin to that found in the subgel phase of the saturated PC analogues (Yager & Schoen, 1984; Schoen & Yager, 1985). These observations were made primarily on the basis of the behavior of the material as revealed by Raman and infrared spectroscopic measurements. This is supported by the present X-ray diffraction results in that for both the subgel phase of the saturated phosphatidylcholines and the L_c phase of sheets and tubules a large number of sharp and diffuse reflections are seen in the intermediate- and wide-angle regions (Yager et al., 1988). Such a wide-angle pattern has been indexed and analyzed in terms of a two-dimensional lattice for the subgel phase of DPPG (Blaurock & McIntosh, 1986). This accounts for the phase designation of lamellar crystalline for the low-temperature form of tubules and sheets. However, the wide-angle diffraction patterns of the subgel phase of the saturated PCs and the hydrated microstructures of $DC_{8,9}PC$ are quite different in terms of number, position, and relative intensity of the various reflections (Caffrey & Hing, 1987). Since the hydrocarbon subcell type or types have not been ascertained on the basis of these limited number of wide-angle reflections, a comparison of the detailed chain packing is not possible. Suffice it to say that on the basis of X-ray diffraction behavior, chain packing within the fully hydrated sheet and tubule microstructures has a crystalline character.

Upon passage through the chain order/disorder transition, dry $DC_{8,9}PC$ undergoes a reduction of 10.8 Å in lamellar d spacing (Table I). This corresponds to a 18.8% decrease in bilayer thickness. Assuming that the model presented in Figure 6A is correct, a reduction in bilayer thickness of ca. 2 Å is expected for methylene segment melting only. This calculation assumes a contribution of 1.00 and 1.26 ± 0.01 Å per methylene group above and below T_t, respectively (Hauser & Shipley, 1983; Tardieu et al., 1973), and accounts for the tilt angle in the L_c phase. In the absence of a high-resolution electron density profile for the L_α phase, an explanation for the observed large reduction in bilayer thickness upon chain melting must, of necessity, remain speculative.

Electron Density Profile. As will be discussed below, the structure of the unit cell for hydrated $DC_{8,9}PC$ tubules does not change significantly upon hydration. Thus, we have been able to construct a high-resolution, one-dimensional electron density profile in the direction normal to the bilayer plane by performing a Fourier analysis of the (00l) diffracted intensities collected by using aligned, multilayer samples equilibrated in an atmosphere of controlled RH and temperature. Such a profile with a resolution of 3.93 Å is presented in Figure 7A. This is the only profile that is consistent with the swelling data and meets the criterion of flatness outlined previously. Any other phase combination gave rise to large fluctuations in the acyl chain region. The profile agrees with the model (Figure 6A) described above based on powder diffraction data. The salient features of the profile are (i) a high electron density peak at ±25.1 Å arising from the electron-rich headgroup, (ii) a single, slightly smaller peak at ±21.4 Å, due to the glycerol backgone, (iii) two relatively flat regions due to the methylene groups of the acyl chains, (iv) a small peak at about ±10.3 Å in the middle of the flat region that has been assigned to the more electron dense diacetylenic moiety, and (v) a large,

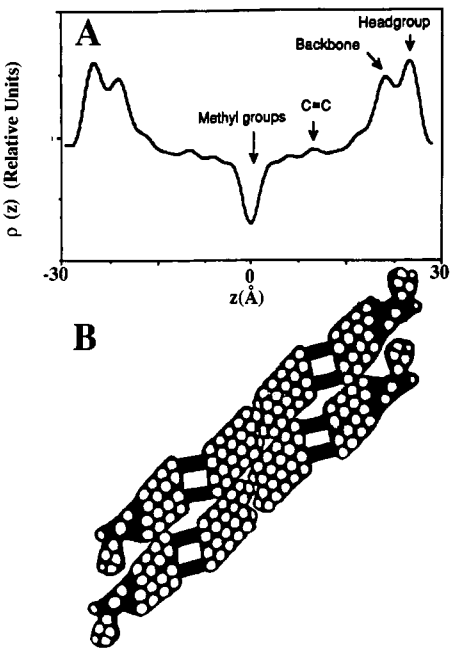

FIGURE 7: One-dimensional electron density profile of $DC_{8,9}PC$ in tubule morphology at 57% RH and 22 °C and at a resolution of 3.93 Å (A). The origin of the various peaks and valleys in the profile is indicated above the profile and is referenced to the proposed molecular conformation of the lipid in the L_C phase of tubules shown in part B. The lamellar repeat spacing under these conditions is 59 Å.

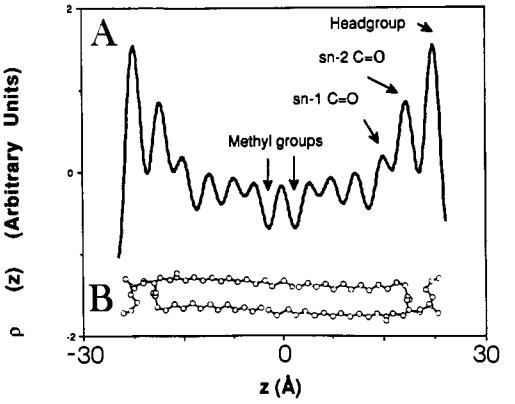

FIGURE 8: One-dimensional electron density profile of the L_C phase of DMPE at a resolution of 3.81 Å. The corresponding molecular conformation of the lipid in the bilayer is shown in part B. The profile was calculated by using the structure factor amplitudes and phase angles provided by Hitchcock et al. (1975). The lamellar repeat distance is 49.5 Å.

single trough at the center of the bilayer due to the terminal methyl groups, which are of low electron density. These features point to certain conditions that must be met by any model for the conformation of the diacetylenic lipid in the L_C phase. At this juncture, it is instructive to compare the electron density profile obtained for $DC_{8,9}PC$ with the corresponding profile of the L_c phase of DMPE at a similar resolution (Figure 8A). The latter was calculated by using the structure factors reported by Hitchcock et al. (1975). A major difference between DMPE and $DC_{8,9}PC$ is apparent in the electron density profile in the vicinity of the glycerol backbone. In DMPE, the backbone peak is split in two due to the staggered arrangement of the carbonyl groups at the *sn*-1 and *sn*-2 positions of glycerol (Figure 8B). For $DC_{8,9}PC$, there exists but a single peak in this region, which is larger in intensity than observed with DMPE. This suggests that in the case of $DC_{8,9}PC$ the carbonyl groups are superimposed when projected

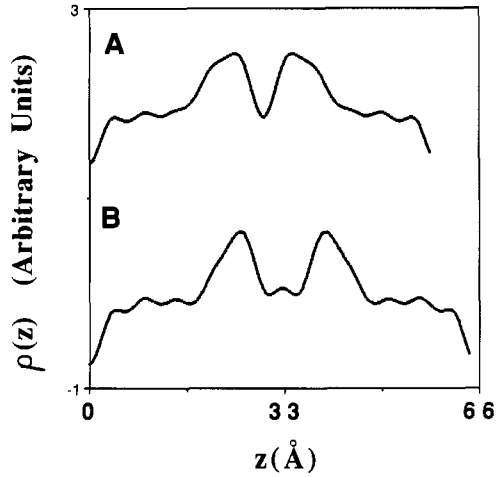

FIGURE 9: Electron density profile of oriented $DC_{8,9}PC$ tubules at 22 °C and at 57% RH (A) and 86% RH (B). To facilitate an evaluation of the effect of hydration changes on structure, the profiles have been drawn with the center of the bilayer at the origin of the abscissa. In part A the lamellar repeat distance is 59.0 Å, the resolution is 5.90 Å, and the distance separating polar headgroups across the interlamellar water space (d_{pol}) is 9.5 Å. The corresponding values for the profile presented in part B are 65.6, 5.96, and 14.3 Å, respectively.

on the bilayer normal. In the acyl chain region the electron density shows pronounced undulations in the L_c phase of DMPE—much more so than in the same region of the diacetylenic lipid. Thus, the projected electron density variation in moving along the hydrocarbon chain appears to be "smeared out" in the case of $DC_{8,9}PC$. This can be accounted for by a tilting of the hydrocarbon chains away from the bilayer normal, which, for the diacetylenic lipid, is calculated to be 36°. The third, and perhaps most noticeable, difference in the two profiles is in the center of the bilayer. We have already noted for $DC_{8,9}PC$ that there is a large, single trough in this region, whereas for DMPE two, shallower troughs are apparent, which are symmetrically positioned about the bilayer midplane. The crystal structure of DMPE indicates that this latter arrangement arises from chain interdigitation to the extent of ca. two methylene units at the bilayer center. Clearly, for $DC_{8,9}PC$ this is not the case. The terminal methyl groups do not significantly interdigitate but rather lie along the midplane of the bilayer. The absence of interdigitation can be effected by a rearrangement of the glycerol backbone and/or by chain tilting, either of which will bring the methyl groups on the *sn*-1 and *sn*-2 chains into registry at the bilayer midplane. A molecular model that incorporates elements of both of these possibilities is presented in Figure 7A. Apart from a small increase of 4° in the calculated tilt angle of the hydrocarbon chains, this is the same conformation as proposed above on the basis of the powder diffraction data and CPK molecular modeling.

The powder diffraction data collected on $DC_{8,9}PC$ in the tubule morphology indicated that chain packing within the bilayers was insensitive to hydration (Table I). The electron density profiles obtained for tubules under different RH conditions corroborate this result (Figure 9). In Figure 9, profiles are presented at similar resolution and with the origin of the profile at the bilayer midplane to facilitate an evaluation of the consequence of adjusting the degree of hydration. At 57% and 86% RH the corresponding *d* spacing values are 59.0 and 65.6 Å, respectively. However, from a perusal of the data in Figure 9 it is apparent that the difference in *d*-spacing value of 6.6 Å arises primarily (to within the resolution limits of the measurement) from an increase in the water layer thickness.

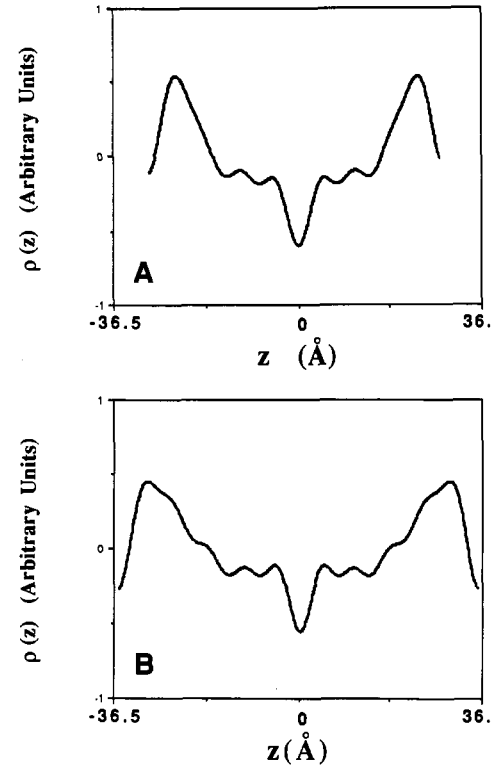

FIGURE 10: Comparison of the one-dimensional electron density profiles for oriented samples of $DC_{8,9}PC$ tubules (A) and of DTPC in the $L_{\beta'}$ phase (B) at 57% RH and 22 °C. In part A the lamellar repeat distance is 59.0 Å, the resolution is 7.38 Å, and the d_{p-p} is 47.8 Å. The corresponding values for the profile shown in part B are 71.4, 7.14, and 59.7 Å, respectively.

The latter increases from 9.5 Å at 57% RH to 14.3 Å at 86% RH. This result shows that with tubules the consequence of increasing the degree of hydration of the lipid is to cause the bilayers to separate without significantly altering the lipid packing arrangement within the bilayer. This physically reasonable behavior lends credance to the structure factor phase assignments as suggested by Torbet and Wilkins (1976).

Comparing $DC_{8,9}PC$ with its saturated analogue DTPC under dry powder conditions at 27–29 °C, we find a lamellar repeat distance difference of 10.5 Å (Table I). At 57% RH, the difference in *d* spacing for aligned multilayer samples amounts to 12.4 Å (Figure 10). From the corresponding electron density profiles it is apparent that the interlamellar water layer thickness, d_w, remains constant at 11–12 Å, regardless of whether the acyl chains of the lipid are saturated or contain a diacetylenic moiety. Thus, the large difference (12.4 Å) in *d* spacing between the two lipids at 57% RH derives primarily from a change in the thickness of the bilayer. The question remains as to the origin of this bilayer thickness difference since both lipids have identical headgroups and acyl chains that are 23 carbons long. Furthermore, for both lipids there exists a single trough in the electron density profile at the bilayer midplane (Figure 10). This suggests that chain interdigitation does not occur where adjoining monolayers meet and that the terminal methyl groups lie in the bilayer midplane. Thus, the difference in bilayer thickness must arise at least in part from the presence of the diacetylenic moiety in $D\text{-}C_{8,9}PC$, which introduces a kink in the chain where no such kink exists in the case of DTPC. From the model presented in Figure 7B we see that the $DC_{8,9}PC$ molecule is tilted some 36° away form the bilayer normal, which has the effect of decreasing bilayer thickness by a factor of 0.19 (1 − cos 36°) compared to the untilted conformation. The data in Figure

10B suggest that the DTPC molecules are tilted also but to a lesser degree than observed with $DC_{8,9}PC$. For example, in this figure the glycerol backbone to glycerol backbone distance (d_{b-b}) is 52.5 Å. This implies a tilt angle of 25 ± 1°, assuming the hydrocarbon chains are in the all-trans configuration with a C–C bond length of 1.26 ± 0.01 Å (Hauser & Shipley, 1983; Tardieu et al., 1973). Thus, the larger bilayer thickness of DTPC compared to $DC_{8,9}PC$ is attributable to a shallower tilt angle and to the possession of fully extended, nonkinked acyl chains.

Molecular Volumes. The partial specific volume data indicate that the introduction of a triple bond at the C10 and C12 positions on the acyl chains of DTPC brings about a reduction in molecular volume by approximately 16 Å^3 per triple bond. Data for ethane/acetylene in the liquid phase at −90 ± 10 °C gave a 17–22 Å^3 volume reduction upon introduction of a triple bond (Weast & Astle, 1977; Marcus, 1977). Thus, the value obtained in this work of 16 Å^3 per triple bond is in reasonable agreement despite the disparate experimental conditions under which these measurements were made. This compaction is reflected in the electron density profiles of the diacetylenic lipid, which show a more electron dense region in the vicinity of the triple bonds (Figure 7A). The partial specific volume data also suggest that a reduction in molecular volume occurs to the extent of ca. 1.2% as the diacetylenic lipid changes morphology from MLVs to tubules. Thus, the lipid molecules appear to pack more tightly in tubules compared to MLVs. Such a difference has not been detected in previous measurements made by IR and Raman spectroscopy (Yager & Schoen, 1984; Rudolph & Burke, 1988) but is consistent with recent fluorescence studies (Plant et al., 1990).

Driving Force for Tubule Formation. Although a growing body of data has been generated on the biophysical characteristics of tubular microstructures formed from diacetylenic phosphatidylcholines, the driving force for the formation of these structures is not well understood. The observation of a high degree of conformational order seems to be a pertinent feature, although this alone is not sufficient to explain the formation of cylinders, since stacked bilayer sheets have a similar degree of conformational order as demonstrated in this and other work (Rudolph & Burke, 1987). Yager et al. have postulated that it is the wrapping or rolling of bilayers during the crystallization event and the unusual packing constraints of $DC_{8,9}PC$ that are responsible for the formation of tubules from this lipid (Yager et al., 1988). Theoretical considerations of the chirality of the lipid and spontaneous torsion of edges of bilayers based on an elastic strain model and the ferroelectric properties of the diacetylenic lipid have both been put forth as possible explanations for tubule assembly (de Gennes, 1987a,b; Helfrich, 1986). Finally, the formation of tubular microstructures from nondiacetylenic amphiphiles suggests that the presence of these functional groups in the acyl chains is not necessary for the formation of a cylindrical morphology (Nakashima et al., 1985; Servuss, 1988; Curatolo & Neuringer, 1986; Fuhrhop & Boettcher, 1990). Thus, the identification of common features at the molecular and nanostructure level that drive tubule formation must await a more complete characterization of these latter systems.

ACKNOWLEDGMENTS

We thank G. W. Feigenson (NIH Grant HL-18255), B. Hummel, P. Schoen, and the entire CHESS (NSF Grant DMR81-12822) and MacCHESS (NIH Grant RR01646) staff for their invaluable help and support.

Registry No. DMPE, 998-07-2; DTPC, 112241-60-8; $DC_{8,9}PC$, 76078-28-9; water, 7732-18-5.

REFERENCES

Blaurock, A. E. (1967) Ph.D. Thesis, University of Michigan.
Blaurock, A. E., & McIntosh, T. J. (1986) *Biochemistry 25*, 299–305.
Buldt, G., Gally, H. U., Seelig, A., & Seelig, J. (1978) *Nature 271*, 182–184.
Burke, T. G., Sheridan, J. P., Singh, A., & Schoen, P. (1986) *Biophys. J. 49*, 321a.
Burke, T. G., Singh, A., & Yager, P. (1988a) *Proc. N.Y. Acad. Sci. 507*, 330–334.
Burke, T. G., Rudolph, A. S., Price, R. R., Sheridan, J. P., Dalziel, A. W., & Singh, A. (1988b) *Chem. Phys. Lipids 48*, 215–230.
Caffrey, M. (1984) *Nucl. Instrum. Methods Phys. Res. 222*, 329–338.
Caffrey, M. (1987) *Biochemistry 26*, 6349–6363.
Caffrey, M., & Hing, F. S. (1987) *Biophys. J. 51*, 37–46.
Chapman, D., Williams, R. M., & Ladbrooke, B. D. (1967) *Chem. Phys. Lipids 1*, 445–475.
Curatolo, W., & Neuringer, L. J. (1986) *J. Biol. Chem. 261*, 17177–17182.
de Gennes, P.-G. (1987a) *C. R. Acad. Sci. Paris 304*, 7–8.
de Gennes, P.-G. (1987b) *C. R. Acad. Sci. Paris 304*, 259–263.
Franks, N. P. (1976) *J. Mol. Biol. 100*, 345–358.
Franks, N. P., & Levine, Y. K. (1981) in *Membrane Spectroscopy* (Grell, E., Ed.) pp 437–487, Springer-Verlag, New York.
Fuhrhop, J.-H. & Boettcher, C. (1990) *J. Am. Chem. Soc.* 112, 1768–1776.
Georger, J. H., Singh, A., Price, R., Schnur, J. M., Yager, P., & Schoen, P. E. (1987) *J. Am. Chem. Soc. 109*, 6169–6175.
Hauser, H., & Shipley, G. G. (1983) *Biochemistry 22*, 2171–2178.
Helfrich, W. (1986) *J. Chem. Phys. 85*, 1085–1088.
Hitchcock, P. B., Mason, R., & Shipley, G. G. (1975) *J. Mol. Biol. 94*, 297–299.
Hupfer, B., Ringsdorf, H., & Schup, H. (1983) *Chem. Phys. Lipids 33*, 355–374.
Johnston, D. S., & Chapman, D. (1985) in *Liposome Technology* (Gregorialas, G., Ed.) Vol. 1, CRC Press, New York.
Johnston, D. S., McLean, L. R., Whitam, M. A., Clark, A. D., & Chapman, D. (1983) *Biochemistry 22*, 3194–3202.
Kim, J. T., Mattai, J., & Shipley, G. G. (1987) *Biochemistry 26*, 6592–6598.
Luzzati, V. (1968) in *Biological Membranes, Physical Fact & Function* (Chapman, D., Ed.) Vol. 1, pp 71–123, Academic Press, New York.
Luzzati, V., Tardieu, A., & Taupin, D. (1972) *J. Mol. Biol. 64*, 269–286.
Marcus, Y. (1977) *Introduction to Liquid State Chemistry*, p 58, Wiley, New York.
McIntosh, T. J., & Simon, S. A. (1986) *Biochemistry 25*, 4058–4066.
McIntosh, T. J., McDaniel, R. V., & Simon, S. A. (1983) *Biochim. Biophys. Acta 731*, 109–114.
Nakashima, N., Asakuma, S., & Kunitake, T. (1985) *J. Am. Chem. Soc. 107*, 509.
O'Brien, F. E. M. (1948) *J. Sci. Instrum. 21*, 73–76.
Plant, A. L., Benson, D. M., & Trusty, G. L. (1990) *Biophys. J. 57*, 925–933.
Regen, S. L., Singh, A., Oehme, G., & Singh, M. (1982) *J. Am. Chem. Soc., 104*, 791–796.

Rhodes, D. G., Blechner, S. L., Schoen, P. E., & Yager, P. (1987) *Biophys. J. 51*, 527a.
Rhodes, D. G., Blechner, S. L., Yager, P., & Schoen, P. E. (1988) *Chem. Phys. Lipids 49*, 39-47.
Rosenblatt, C., Yager, P., & Schoen, P. E. (1987) *Biophys. J. 52*, 295-301.
Rudolph, A. S., & Burke, T. G. (1987) *Biochim. Biophys. Acta 902*, 349-359.
Rudolph, A. S., Burke, T. G., & Sheridan, J. P. (1987) *Biophys. J. 51*, 185a.
Sayre, D. (1952) *Acta Crystallogr. 5*, 843.
Schnur, J. M., Price, R., Schoen, P., Yager, P., Calvert, J. M., Georger, J., & Singh, A. (1987) *Thin Solid Films 152*, 181-206.
Schoen, P. E., & Yager, P. (1985) *J. Polym. Sci., Polym. Phys. Ed. 23*, 2203-2216.
Schoen, P. E., Yager, P., Sheridan, J. P., Price, R., Schnur, J. M., Singh, A., Rhodes, D. G., & Blechner, S. L. (1987) *Mol. Cryst. Liq. Cryst. 153*, 357-366.
Servuss, R. M. (1988) *Chem. Phys. Lipids 46*, 37-41.
Shannon, C. E. (1949) *Proc. Inst. Radio Eng. N.Y. 37*, 10-21.
Sheridan, J. P. (1988) *Nav. Res. Lab. Memo. Rep.* 5975.
Singh, A., Thompson, R. B., & Schnur, J. M. (1986) *J. Am. Chem. Soc. 108*, 2785.
Snyder, R. G., Hsu, S. L., & Krimm, S. (1978) *Spectrochim. Acta 34a*, 395.
Tardieu, A., Luzzati, V., & Reman, F. C. (1973) *J. Mol. Biol. 75*, 711-733.
Torbet, J., & Wilkins, M. H. F. (1976) *J. Theor. Biol. 62*, 447-58.
Weast, R. C., & Astle, M. J., Eds. (1977) *CRC Handbook of Chemistry and Physics*, CRC Press, Boca Raton, FL.
Yager, P., & Schoen, P. (1984) *Mol. Cryst. Liq. Cryst. 106*, 371-381.
Yager, P., Schoen, P. E., Davies, C., Price, R., & Singh, A. (1985) *Biophys. J. 48*, 899-906.
Yager, P., Price, R. P., Schnur, J. M., Schoen, P. E., Singh, A., & Rhodes, D. G. (1988) *Chem. Phys. Lipids 46*, 171-179.

On the Use of Deuterium Nuclear Magnetic Resonance as a Probe of Chain Packing in Lipid Bilayers†

N. Boden,* S. A. Jones, and F. Sixl
School of Chemistry, The University, Leeds LS2 9JT, U.K.
Received July 10, 1990; Revised Manuscript Received November 2, 1990

ABSTRACT: The packing of hydrocarbon chains in the bilayers of lamellar (L_α) phases of soap/water and phospholipid/water mixtures has been studied by deuterium NMR spectroscopy and X-ray diffraction. A universal correlation is shown to exist between the average C-D bond order parameter $\bar{S}_{CD}$ of hydrocarbon chains and the average area per chain a_{ch}, irrespective of the chemical structure of the surfactant (hydrophilic group, number of chains per molecule, and chain length), composition, and temperature. The practical utility of the correlation is illustrated by its application to the characterization of the distribution of various hydrophobic and amphiphilic solutes in bilayers. The distribution of hydrocarbons within a bilayer is shown to depend upon their molecular structure in a manner which highlights the nature of the molecular interactions involved. For example, benzene is shown to be fairly uniformly distributed across the bilayer with an increasing tendency to distribute into the center at high concentrations. In contrast, the more complex hydrocarbon tetradecane preferentially distributes into the center of the bilayer at low concentrations, while at higher concentrations it intercalates between the surfactant chains. Alcohols such as benzyl alcohol, octanol, and decanol all interact similarly with the bilayer in so far as they are pinned to the polar/apolar interface, presumably by involvement of the hydroxyl group in a hydrogen bond. But the response of the surfactant chains to the void volume created in the center of the bilayer is dependent upon the distance of penetration of the alcohol into the bilayer. For benzyl alcohol, the shortest molecule, this void volume is taken up by the disordering of the chains, while for decanol, the longest molecule, it is absorbed by interdigitation of the chains of apposing monolayers. For octanol, the chain interdigitation mechanism is dominant at low concentrations, but there is a transition to chain disordering at high concentrations. Finally, it is shown that the correlation provides a useful test for statistical mechanical models of chain ordering in lipid bilayers.

Membranes are quasi two-dimensional, multicomponent fluids. The underlying structural element is a bimolecular layer of amphiphilic lipids. This bilayer has consequently been the subject of extensive experimental and theoretical studies. It consists of a core of hydrocarbon chains which is separated from the water by a layer of densely packed hydrophilic headgroups. The packing density of the hydrocarbon chains within the bilayer is commonly described in terms of either the bilayer thickness d_l or the average area per molecule a_m at the bilayer/water interface. Most of our knowledge concerning molecular packing in lipid bilayers has been obtained from X-ray measurements of the bilayer repeat distance d_o in lamellar L_α phases according to a procedure first described by Luzzati (1969): d_l is calculated from $d_l = \phi_l d_o$ and a_m from $a_m = 2V_l/Nd_l$, where ϕ_l, V_l, and N are respectively the volume fraction of lipid, the partial molar volume of lipid, and the

† We thank the University of Leeds for a "Pool Post" for F.S. and the Science and Engineering Research Council for a research studentship to S.A.J. and for financial support to purchase equipment.

0006-2960/91/0430-2146$02.50/0